Journal of Applied Electrochemistry **31**: 245–250, 2001.

Electrochemical studies of the nickel electrode with cobalt modification

A.B. YUAN* and N.X. XU
Shanghai Institute of Metallurgy, Chinese Academy of Sciences, Shanghai 200050, P.R. China
*(*author for correspondence, e-mail: abyuan@sina.com)*

Received 1 June 2000; accepted in revised form 22 August 2000

Key words: alkaline storage battery, electroless deposition of cobalt, interface conduction, nickel electrode, nickel foam

Abstract

The electrochemical behaviour of the paste-type nickel hydroxide electrode with cobalt-modified nickel foam was investigated using galvanostatic charge–discharge, electrochemical impedance spectroscopy, cyclic voltammetry and current pulse relaxation methods. Experimental results showed that the performance of the nickel electrode with substrate deposition of a thin layer of cobalt was improved markedly. This improvement could be attributed to the enhanced electrical conduction between the substrate and the active material. The enhanced electrical conduction increases the charge efficiency and the discharge depth of the nickel electrodes and therefore increases the utilization of the active material. This suggests that the electrical conduction between the substrate and the active material is essential to the practical use of paste-type nickel hydroxide electrodes.

1. Introduction

The nickel hydroxide electrode, used as positive electrode in rechargeable alkaline batteries such as Ni/Cd and Ni/Zn, has been the subject of many fundamental and practical studies. In recent years, its new application to Ni/MH batteries has received more attention. In conventional Ni/Cd batteries, the positive nickel electrodes are manufactured from sintered plates. Foamed nickel electrodes have been employed as positive electrodes in Ni/MH batteries because of their high specific energy and low cost. In current designs of rechargeable nickel batteries, the battery capacity is generally limited by the nickel electrode. Hence, increasing the energy density of the nickel electrode is essential to increase the energy density of the whole battery.

The nickel electrode reaction can be expressed as

$$Ni(OH)_2 + OH^- \rightleftharpoons NiOOH + H_2O + e^- \quad (1)$$

which can be viewed as a proton intercalation/deintercalation reaction in the solid [1–4]. When the electrode is charged, nickel hydroxide is oxidized to nickel hydroxyl. During discharging, the reaction is reversed. According to Tuomi [5], the charged form NiOOH is an n-type semiconductor, while the reduced product $Ni(OH)_2$ is a p-type semiconductor. Zimmerman and Effa [4] indicated that, under normally high rate discharge conditions, the kinetics of nickel electrode discharge are controlled by solid-state proton diffusion. As discharge proceeds, the conductivity of the active material decreases gradually until eventually mixed kinetics are observed where the proton diffusion and charge transfer are both contributing to the total electrode reaction. Further discharge results in the formation of a semiconductor layer at the interface of current collector and active material, and the layer is depleted in charge carriers and has a relatively high electric resistance. The diffusion rate and concentration of protons are expected to depend on the phase composition of the NiOOH, as well as on the presence of additives in the lattice structure. Cobalt has been found to increase the ionic and electronic conductivity of the active material and to result in a greater depth of discharge before depletion layer formation.

The effects of coprecipitated cobalt hydroxide on the electrochemical performance of the nickel hydroxide electrode has been documented [6–9]. For paste-type nickel electrodes, beside the modification of the material by chemical coprecipitation of cobalt and zinc, another effective method is the physical addition of cobalt compounds or cobalt metal powder to the nickel hydroxide [10, 11]. To make full use of elemental cobalt, the surface of the nickel hydroxide powder can be microencapsulated with a thin layer of cobalt by electroless deposition [12], which increases the active material utilization of the Ni electrode. However, this treatment is rather tedious. In the present work, an alternative approach of cobalt modification for the nickel electrode by electroless deposition of cobalt on nickel foam is proposed and the effects of such modification and cobalt powder addition on nickel electrode performance were studied using electrochemical methods.

2. Experimental details

2.1. *Nickel electrode preparation*

Nickel foam substrates of dimensions of 2 cm × 2 cm × 0.16 cm and porosity of 95% with a spot-welded nickel ribbon were covered with a thin layer of cobalt by electroless deposition and the deposited cobalt weighted about 0.026 g. As-received nickel foam was also used for comparison. 0.4 g nickel hydroxide (Westaim Corp. 6766, Canada, with coprecipitation of zinc and cobalt) with or without 5 wt % cobalt powder addition were mixed. Then the 5 wt % PTFE dispersion was added and mixed. The pasty mixture was incorporated into the above-mentioned substrates using a spatula, and then dried at 65 °C and roll pressed to 0.5 mm thick.

2.2. *Electrochemical measurements*

The as-prepared nickel electrodes were activated for three cycles prior to the electrochemical measurements. The activation, charging–discharging at different rates and cycle life tests were conducted in a three-electrode system by an automatic cycler (model DC-5) controlled by a microcomputer. The nickel electrode under test was used as working electrode. The counter electrode was a metal hydride electrode with excess capacity. The electrolyte was 6 M KOH aqueous solution. A Hg/HgO electrode with the same alkaline solution was employed as the reference electrode.

Electrochemical impedance spectroscopy (EIS) measurements were performed using a Solartron 1255B frequency response analyser coupled with a 1287 electrochemical interface in conjunction with Zplot 2 software. All measurements were conducted at open circuit potential (OCP) and at 20 °C. Cyclic voltammetry (CV) and current pulse relaxation (CPR) measurements were performed using a Solartron SI 1287 electrochemical interface in conjunction with CorrWare 2 software.

3. Results

3.1. *Specific discharge capacity and cycle life of nickel electrodes*

Table 1 indicates that the specific discharge capacity of the nickel hydroxide electrode with as-received nickel foam is fairly low. In contrast, the capacities of the electrode with electroless cobalt modified nickel foam at various charge-discharge rates are about 50 mAh g^{-1} higher than the untreated one. For the as-received nickel foam, 5 wt % cobalt powder addition to the paste also increases the capacity, but the increase is slightly less remarkable than for the nickel foam modification. Furthermore, the capacity difference between the foam-modified and the paste-modified electrodes decreases with the increase of charge-discharge rate.

Table 1. Specific discharge capacity at various charge–discharge rates and recovery potential of various nickel electrodes

Nickel hydroxide electrode	$C_{0.1C}$	$C_{0.2C}$	$C_{0.4C}$	C_{1C}	Recovery potential /V
	/mAh g^{-1} $Ni(OH)_2$				
As received Ni foam + plain $Ni(OH)_2$ (Bare)	218	172	158	137	0.357
Co deposited Ni foam + plain $Ni(OH)_2$ (Treated)	272	229	210	184	0.349
As received Ni foam + Co powder added $Ni(OH)_2$ (Co added)	251	223	206	183	0.351
Co deposited Ni foam + Co powder added $Ni(OH)_2$ (Treated + Co added)	281	254	237	215	0.346

This suggests that cobalt powder addition is more beneficial at higher charge-discharge rates. Among the four types of nickel electrodes under study, the electrode by combination of substrate modification and cobalt powder addition exhibits the highest discharge capacity, about 80 mAh g^{-1} higher than the bare one with the exception of 63 mAh g^{-1} higher at 0.1 *C* rate. Besides, the capacity differences between the two electrodes with cobalt powder addition at different charge-discharge rates are almost the same (i.e., 30 to 32 mAh g^{-1}).

In the present studies the capacity variation with different electrodes seemed to be consistent with their variation of recovery potential after discharged to 0.1 V (cut-off potential) at *C*/10 rate. According to some researches [13–16], the equilibrium potential of nickel electrode is a function of the state of charge (SOC). Approximately, the open circuit potential (OCP or quasi-equilibrium potential) of the nickel electrode could be viewed as an indicator for the SOC. The lower recovery potential suggests the higher discharge depth.

The charge–discharge cycle life test results are displayed in Figure 1. For the nickel electrode with no modification, the discharge capacity deterioration with cycling is fast, dropping from 136 to 59 mAh g^{-1} through 200 cycles. The cycling property of the modified electrodes is considerably improved, especially for the electrode with substrate modification and cobalt addition.

3.2. *EIS study*

Conclusions can be obtained from the a.c. impedance measurement results (Figures 2–4) that (i) at discharged state (0% SOC), the impedance of the bare electrode is much greater than that of the others. At 50% and 100% SOCs, the differences between the various electrodes are much smaller compared to that at 0% SOC; and (ii) from 0% to 50% SOCs, the impedance of the electrodes change markedly, especially for the bare one. From 50% SOC to 100% SOC, the impedance plot does not change much.

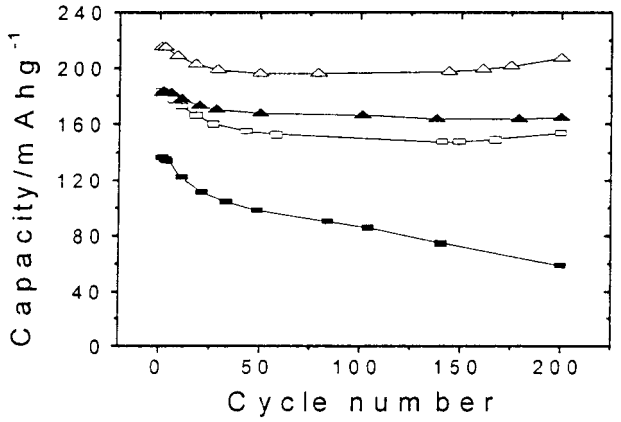

Fig. 1. Specific discharge capacity of the nickel electrodes as a function of cycle number at 1*C* charge–discharge rate. Key: (■) bare, (□) treated, (▲) Co added and (△) treated + Co added.

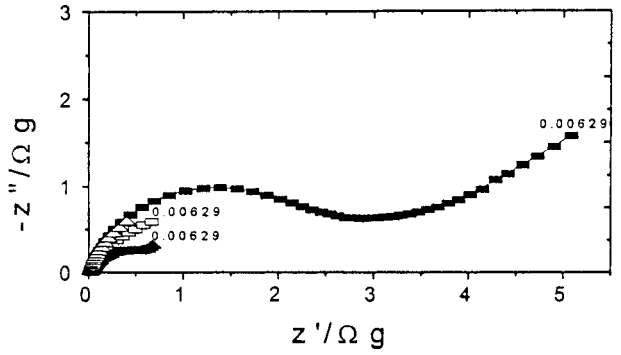

Fig. 2. Nyquist plot for the electrodes at 0% SOC after activation. Key: (■) bare, (□) treated, (▲) Co added and (△) treated + Co added.

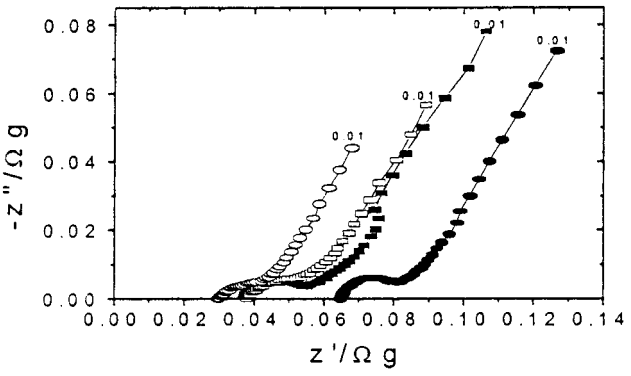

Fig. 3. Nyquist plot for the electrodes at 50% SOC after activation. Key: (■) bare, (□) treated, (●) Co added and (○) treated + Co added.

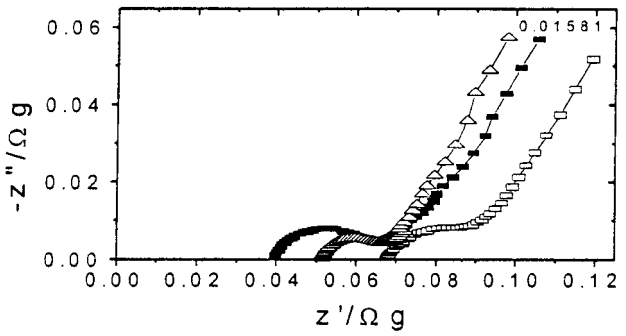

Fig. 4. Nyquist plot for the electrodes at 100% SOC after activation. Key: (■) bare, (□) treated and (△) Co added.

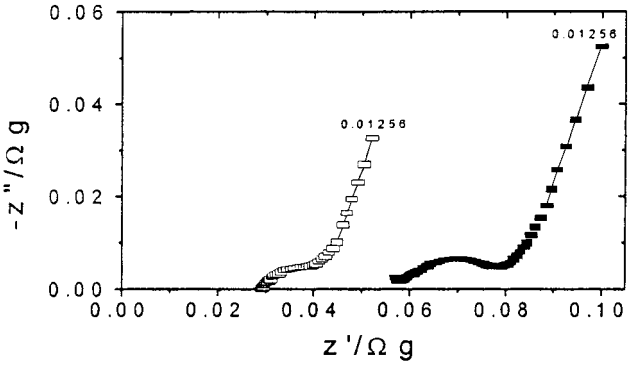

Fig. 5. Nyquist plot for the electrodes at 50% SOC after 200 cycles at 1C rate. Key: (■) bare and (□) treated + Co added.

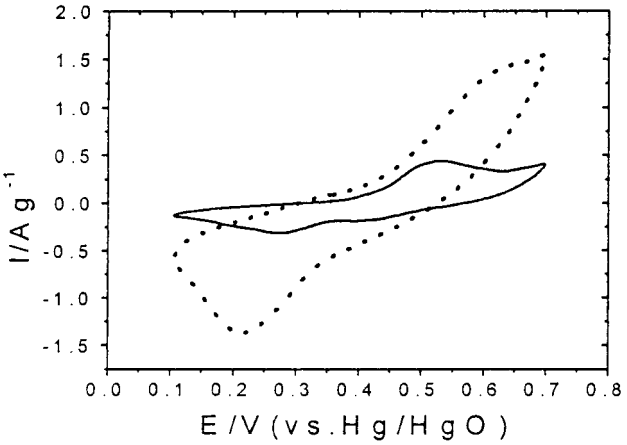

Fig. 6. Cyclic voltammograms of the bare and modified nickel electrodes at scan rate of 1 mV s^{-1}. Key: (—) bare and (····) treated + Co added.

The impedance plots for the bare and modified electrodes at 50% SOC after 200 cycles are shown in Figure 5. It can be seen from comparison of Figure 3 and Figure 5 that the electrode impedance changed little through 200 charge–discharge cycles.

3.3. *Cyclic voltammetry*

Comparison of cyclic voltammetry results (Figure 6) shows that the peak current of the electrode with cobalt powder addition and surface modification of the substrate with cobalt is much larger than that without cobalt. This result reflects the redox activities of the two electrodes (discussed later).

Owing to the slow diffusion of proton in nickel electrode, the normal Tafel plots could not be used effectively to measure the exchange current density and charge transfer coefficient of the nickel electrode. When the polarization current is larger than the exchange current, the electrochemical reactions are controlled by

both charge transfer and mass transfer processes. The cathodic overpotential can be expressed as [17]

$$\eta = \frac{RT}{\alpha F}\ln\frac{i_L}{i_0} + \frac{RT}{\alpha F}\ln\frac{i}{i_L - i} \quad (2)$$

where η is the overpotential, R the gas constant, T the absolute temperature, F the faradaic constant, α the charge transfer coefficient, i_0 the exchange current density, i the polarization current density and i_L the limiting current density.

From Equation 2, the relationship between η and $\ln(i/(i_L - i))$ should be linear. The plots of η against $\ln(i/(i_L - i))$ from cathodic polarization (in Figure 6) are shown in Figure 7. From the slope and intercept of the straight line in the middle range of the derived curves, the kinetic parameters i_0 and α can be obtained. The fitted results are presented in Table 2. The calculated α for the modified electrode is smaller than the bare one, whereas the calculated i_0 for the modified electrode is much larger than the bare one.

The I/E responses of the bare and modified electrodes at different scan rates are illustrated in Figure 8(a) and Figure 8(b), respectively. Both the reaction peak currents and peak potentials are proportional to the scan rates. This suggests some irreversible characteristics for the nickel electrode reaction. Therefore, for a spherical electrode, the following equation should be used [17].

$$i_L = 0.4958\frac{3}{r\rho}nF\left(\frac{\alpha n_\alpha F}{RT}\right)^{1/2} C^0 D^{1/2} v^{1/2} \quad (3)$$

where i_L is the limiting current density (A g^{-1}), r the radium of nickel oxide (cm), ρ the density of nickel oxide (g cm^{-3}), α the charge transfer coefficient, n_α the number of electrons transferred up to and including the rate determining step, C^0 the initial concentration of oxidant (here the concentration of nickel hydroxyl is in mol cm^{-3}), D the diffusion coefficient of proton (cm^2 s^{-1}) and v the scan rate (V s^{-1}).

Table 2. Fitted results of kinetic parameters for the bare and modified electrodes

Nickel electrodes	Intercept	Slope	i_L/A g^{-1}	α	i_0/A g^{-1}
Bare	0.123 73	0.049 94	0.3129	0.5058	0.026 26
Treated + Co added	0.205 01	0.103 86	1.3760	0.2432	0.191 14

The relationship of i_L against $v^{1/2}$ for the bare and modified electrodes are shown in Figure 9. The slope for the modified electrode is much larger than that for the bare one and the reason for this may be explained by analysing the slope-term in Equation 3. The parameters, r, ρ, n and D are constant for these two whereas the terms αn_α and C^0 are different. Although the transfer coefficient α for the modified electrode is smaller than that for the bare one as indicated in Table 2, the initial reactant concentration C^0 for the modified electrode is much larger than that for the bare one. The concentration C^0 is proportional to the discharge capacity of a rechargeable electrode, which can be expressed appropriately as follows [18]

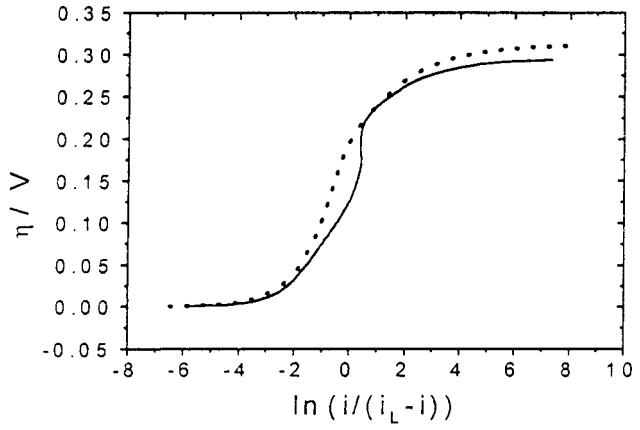

Fig. 7. Overpotential, η, of the bare and modified nickel electrodes as a function of $\ln(i/(i_L - i))$. Key: (—) bare and (···) treated + Co added.

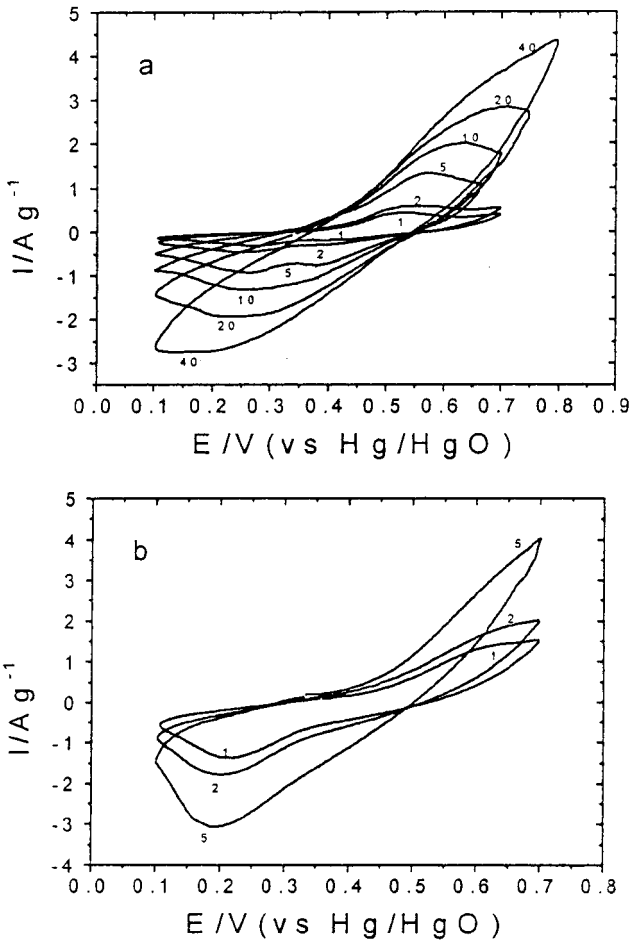

Fig. 8. Cyclic voltammograms of: (a) the bare and (b) substrate modification and cobalt addition nickel electrodes at scan rates of: (a) 1, 2, 5, 10, 20, 40 and (b) 1, 2, 5 mV s^{-1}.

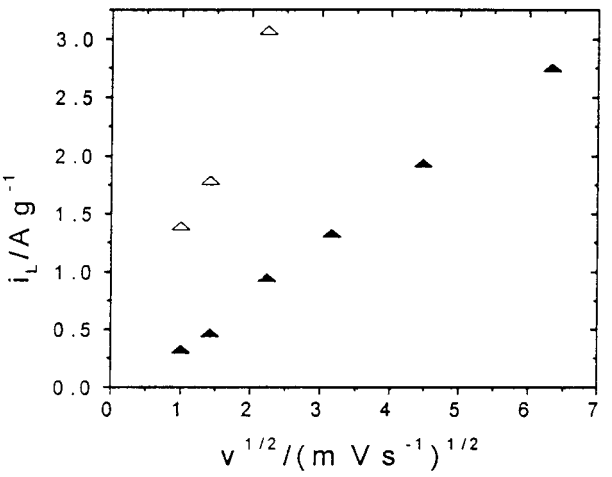

Fig. 9. Limiting current of the bare and modified nickel electrodes as a function of $v^{1/2}$. Key: (▲) bare and (△) treated + Co added.

$$C^0 = 3600\frac{C_{\text{cap}}\rho}{F} \tag{4}$$

where C_{cap} is the discharge capacity (Ah g^{-1}).

3.4. *Current pulse relaxation measurements*

The impedance of a typical electrode process generally consists of three components: namely, ohmic resistance, activation impedance and mass transfer impedance. The set-up and degradation rates of these three polarization processes are entirely different. In general the generation or degeneration of ohmic polarization is very fast, the activation is slower than the ohmic and the diffusion is the slowest. For a nickel hydroxide electrode, the three components of impedance can be separated by current pulse relaxation (CPR) technique (Figure 10). In the case of 0% SOC, the ohmic resistance (the vertical drop or rise in voltage) are rather large, while in the case of 50% SOC, the ohmic resistance is smaller. By comparison of Figure 10(a) and (b), the ohmic and charge transfer polarizations for the two electrodes are very different. Except for the initial period (ohmic and electrochemical relaxation), the time dependence of potential relaxation in the rest time (diffusion relaxation) seems similar. This suggests a similar diffusion behavior of the two electrodes. By interruption of the current pulse, the potentials of the nickel electrode recovered gradually toward an equilibrium state. This is caused by slow diffusion of protons in the solid state. In principle, the proton diffusion coefficient D could be obtained from following formula [19]

$$\Delta E = \frac{IV_{\text{m}}\tau(\text{d}E/\text{d}n)}{FA(\pi Dt)^{1/2}} \tag{5}$$

where ΔE is the time dependence of transient voltage, I the current pulse, V_{m} the molar volume (22.61 cm^3, by assuming the sample as β-nickel hydroxide), τ the duration of the pulse, (dE/dn) the slope of the open circuit voltage against electron transfer number (n = 0 $\sim$ 1 is used by assuming the reaction of nickel electrode being a single electron exchange reaction), F the faradaic constant, A the surface area, and t the relaxation time.

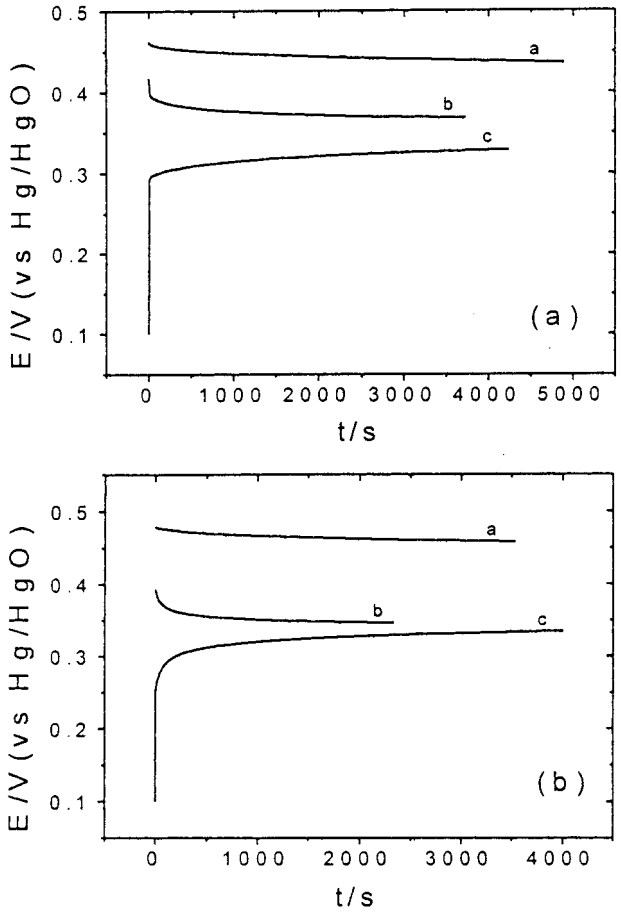

Fig. 10. Potential response in current pulse relaxation measurement for: (a) the bare and (b) modified nickel electrode. In (a) and (b): a, b and c indicate, charged 5 min with 10 mA at 50% SOC, charged 5 min with 10 mA at 0% SOC and discharged with 10 mA to 0.1 V, before current interruption, respectively.

It is necessary to note that the proton diffusion coefficient for nickel electrode cannot be determined accurately by the CPR technique because of the difficulty of definition of the effective surface area of the powder pressed electrode. However, this method could be used to estimate the value of diffusion coefficient in some applications. The similar diffusion behaviour of the two electrodes shows that the cobalt modification does not change the chemical diffusion coefficient of proton.

4. Discussion

From the capacity results in Table 1 it is known that surface microencapsulation of foamed nickel with a thin layer of cobalt increases the specific capacity of the nickel electrode markedly. The redox reactions of the nickel electrode can be viewed as a proton intercalation–deintercalation in solid state with company of electron exchanging [1–4, 20]. On discharging, the reaction

kinetics are generally controlled by the slow diffusion of protons. But, toward the end of discharge the poor conductivity of the reduced nickel hydroxide becomes an essential factor that terminates the discharging. The impedance measurement (Figure 2) showed that in the discharged state, the nickel electrode with no modification has large impedance. With surface modification of the substrate, the electrode impedance decreases dramatically. Substrate modification with cobalt increases the conductance of the nickel electrode via following mechanism [11]

$$Co + 2\,OH^- \rightarrow Co(OH)_2 + 2\,e^- \quad (6)$$

$$Co(OH)_2 + OH^- \rightarrow CoOOH + H_2O + e^- \quad (7)$$

During charging of the nickel electrode, the deposited cobalt layer on the substrate surface can be oxidized to cobalt hydroxyl, which cannot be reduced during subsequent discharging. Such formed cobalt hydroxyl layer with higher conductance provides a good electric path through the interface of substrate and active material, thereby increases the depth of discharge and subsequently the utilization of active material.

The mechanism of improvement of the nickel electrode with physical addition of cobalt is similar to the above discussed, but with conduction improvement between the material articles instead of substrate and active material. From the capacity test results, the effect of substrate modification with cobalt was better than that with addition of cobalt powder into the paste. This suggests that the improvement of conduction between the substrate and active material is more essential. Of course, the effect by combination of substrate modification and cobalt addition is the best. The addition of cobalt powder to nickel electrode is beneficial to the charge–discharge cycles at 1C rate (Figure 1). This can be explained as follows. When the charge–discharge current is not high, the contact resistance between the substrate and active material is dominant; when the current is higher, the contact resistance between active material particles becomes important.

A.c. impedance (Figures 2–4) and current pulse relaxation (Figure 10) results showed that the polarization impedance of the nickel electrode in the discharged state is much higher than that in the charged state (in our work the linear polarization results are also consistent with this result). This is because at discharged state, the reduced product $Ni(OH)_2$ is a p-type semiconductor with poor conductivity; when the electrode is charged, the oxidized product NiOOH is an n-type semiconductor, with conductivity much higher than that of $Ni(OH)_2$ [5, 20].

Cyclic voltammetry results and analyses (Figures 6–8) indicated that the exchange current density of the nickel electrode could be increased apparently by modification with cobalt. This may be interpreted on the basis that the electrocatalysis activity of nickel electrode is increased in the presence of cobalt. The presence of cobalt at the interface between substrate and active material and between active material particles increases the effective surface area or reactive site.

5. Conclusions

Nickel foam substrate modification with a thin layer of electroless coated cobalt can increase the active material utilization of nickel electrode remarkably, typically from 218 to 272 mAh g^{-1} at a charge–discharge rate of $C/10$.

By combination of electroless cobalt deposition on nickel foam and cobalt addition into the active material, the nickel electrode exhibits the highest discharge capacity and the longest cycle life even at higher charge–discharge rate. Almost no capacity deterioration is observed through 200 charge–discharge cycles.

The increase in conduction both between substrate and active material and between active material grains by modification is responsible for the property improvement of the nickel electrodes studied by electrochemical methods.

References

1. P.D. Lukovtsev and G.J. Slaidin, *Electrochim. Acta* **6** (1962) 17.
2. Z. Takehara, M. Kato and S. Yoshizawa, *Electrochim. Acta* **16** (1971) 833.
3. K. Micka and I. Rousar, *Electrochim. Acta* **27** (1982) 765.
4. A.H. Zimmerman and P.K. Effa, *J. Electrochem. Soc.* **131** (1984) 709.
5. D. Tuomi and G.J.B. Crawford, *J. Electrochem. Soc.* **115** (1968) 450.
6. D.F. Pickett and J.T. Maloy, *J. Electrochem. Soc.* **125** (1978) 1026.
7. A.K. Sood, *J. Appl. Electrochem.* **16** (1986) 274.
8. R.D. Armstrong, G.W.D. Briggs and E.A. Charles, *J. Appl. Electrochem.* **18** (1988) 215.
9. A. Audemer, A. Delahaye, R. Farhi, N. Sac-Epée and J-M. Tarascon, *J. Electrochem. Soc.* **144** (1997) 2614.
10. M. Oshitani, H. Yufu, K. Takashima S. Tsuji and Y. Matsumaru, *J. Electrochem. Soc.* **136** (1989) 1590.
11. A.B. Yuan, S.A. Chang, J.Q. Zhang and C.N. Cao, *J. Power Sources* **77** (1999) 178.
12. A.B. Yuan, Doctorate thesis, Zhejiang University, China (1999).
13. M. Jain, A.L. Elmore, M.A. Matthews and J.W. Weidner, *Electrochim. Acta* **43** (1998) 2649.
14. M.S. Suresh, A. Subrahmanyam and K. Usha, *J. Power Sources* **56** (1995) 171.
15. K. Watanabe and N. Kumagai, *J. Power Sources* **66** (1997) 121.
16. K. Watanabe and N. Kumagai, *J. Power Sources* **76** (1998) 167.
17. A.J. Bard and L.R. Faulkner, 'Electrochemical Methods – Fundamentals and Applications' (J. Wiley & Sons, New York, 1980).
18. M.M. Geng, J.W. Han, F. Feng and D.O. Northwood, *J. Electrochem. Soc.* **146** (1999) 3591.
19. K. Watanabe and T. Kikuoka, *J. Appl. Electrochem.* **25** (1995) 219.
20. G. Barral, S. Maximovitch and Njanjo-Eyoke, *Electrochim. Acta* **41** (1996) 1039.